Supplementary Material

2.5D Mass Spectrometry Imaging of N-Glycans In Esophageal Adenocarcinoma and Precursor Lesions

D. R. N. Vos[1,2], S. L. Meijer[3], R.E. Pouw[4], S. R. Ellis[1,5], R. M. A. Heeren[1], B. Balluff[1,*]

Author's affiliations

[1] The Maastricht MultiModal Molecular Imaging Institute (M4I), Maastricht University, Maastricht, The Netherlands

[2] Center for Mass Spectrometry and Optical Spectroscopy (CeMOS), Mannheim University of Applied Sciences, Mannheim, Germany

[3] Department of Pathology, Amsterdam UMC, University of Amsterdam, Amsterdam, The Netherlands

[4] Department of Gastroenterology and Hepatology, Amsterdam UMC, University of Amsterdam, Amsterdam, The Netherlands

[5] Mass Spectrometry Imaging Laboratory, School of Chemistry and Molecular Bioscience, University of Wollongong, Australia

ORCID

RE Pouw: 0000-0002-4707-1186

SL Meijer: 0000-0002-6953-2406

SR Ellis: 0000-0002-3326-5991

RMA Heeren: 0000-0002-6533-7179

B Balluff: 0000-0003-0351-240X

*** Corresponding author:**

Dr. Benjamin Balluff, Maastricht University, Maastricht MultiModal Molecular Imaging institute (M4I), Universiteitssingel 50, P.O. Box 616, 6200 MD Maastricht, The Netherlands; Phone: +31 43 388 1251; Email: b.balluff@maastrichtuniversity.nl

1. Determination of the identity of the statistically significant glycan signals

In order to confirm the assigned identities of the eight N-glycan signals of interest, we have performed high-mass resolution mass spectrometry as well as MS/MS experiments directly *on tissue* using MALDI. These experiments were done on two of the advanced stage samples (patients SAA and SH, see Table 1) since signal intensities of our glycans of interest increased with the progression of the disease. These two samples were also selected since they more mostly homogeneous in their cellular composition by consisting predominantly of tumor cells. The sample preparation has been performed the same way as for any of the mass spectrometry imaging experiments.

a. High-mass resolution mass spectrometry

A high-mass resolution mass spectrum was obtained directly from one of the tissues using MALDI on a Bruker Solarix 9.4T FTICR (Bruker Daltonics GmbH, Germany). The mass range was *m/z* 880–3500 in positive polarity mode with 1E6 data points yielding a resolution of R=150,000 @ *m/z* 1500. MALDI laser was operated at 2000Hz, 65% laser energy, with a small laser focus profile and the accumulation of 500 laser shots per spectrum. The system was previously calibrated using red phosphorus and the quadrupole was set to suppress *m/z* values below 900.

The acquired spectrum (available as supplementary data file "High-mass resolution glycan spectrum.zip") was recalibrated after acquisition using four CHCA matrix signals ($[5M+6Na-5H]^+$, $[6M+7Na-6H]^+$, $[7M+8Na-7H]^+$, and $[8M+9Na-8H]^+$) spanning the range *m/z* 1000–1700. This was done in the software DataAnalysis v.5.3 (Bruker Daltonics GmbH, Germany) using a linear function and a tolerance of 0.02 Da, which yielded a standard deviation of the mass errors of 0.802 ppm. Peak picking was performed in DataAnalysis too using the "FTMS" algorithm and an absolute intensity threshold of 30,000.

The results show that most of the masses correspond to the theoretical mass by less than one ppm; with exception of m/z 2028.73 with a still acceptable error of 2.5 ppm (Table SM1).

Table SM1: Results of high-mass resolution MALDI MS measurements

Detected *m/z* TOF	**Theoretical monoisotopic *m/z***	**Adduct**	**Detected *m/z* FTICR**	**Difference [ppm]**	**Glycan**
933.33	933.317	1 Na	933.31733	0.354	Hex3HexNAc2
1095.37	1095.3698	1 Na	1095.36911	-0.630	Hex4HexNAc2
1419.44	1419.4755	1 Na	1419.47461	-0.627	Hex6HexNAc2
1581.53	1581.5283	1 Na	1581.52692	-0.873	Hex7HexNAc2
1743.56	1743.5811	1 Na	1743.57958	-0.872	Hex8HexNAc2
2028.73	2028.7136	1 Na	2028.70855	-2.489	Hex6HexNAc5
2341.84	2341.7909	2 Na - H	2341.78901	-0.807	Hex6HexNAc5NeuAc1
2393.9	2393.8458	1 Na	2393.84701	0.505	Hex7HexNAc6

b. MS/MS

To obtain more certainty on the assigned identities, these experiments were complemented by further *on tissue* MS/MS experiments. These were done on a timsTOF flex (Bruker Daltonics GmbH, Germany) operated in positive polarity and in the mass range *m/z* 150–2500, as calibrated in MS mode using red phosphorus (standard deviation of error 0.169 ppm). Then mode was switched to MS/MS mode. Fragmentation spectra were acquired for

each parent ion/glycan with a ±5 Dalton window width, a varying CID energy (Table SM2), a laser power 52%, and the laser profile "MS/MS". 6000 laser shots were summed at 1000Hz frequency, which allowed moving across the tissue for a few seconds to obtain more parent ion material.

Peak picking was done in DataAnalysis v.5.3 (Bruker Daltonics GmbH, Germany) with the SNAP algorithm (S/N>2, quality factor>0.9, charge≤2) to exclude isotopic peaks. The peak lists were exported as .mgf files and imported for annotation to the GlycoWorkbench (v. 2.1 stable build 146). Annotations were performed with a 200 ppm tolerance, maximum three cleavages, and maximum 1 (positive) charge. The results are summarized in Table SM2 and show that the coverages range from 23 % (Hex4HexNAc2) to 42 % (Hex6HexNAc2).

Table SM2: Results of GlycoWorkbench annotations of MS/MS measurements

Parent ion [*m/z*]	**CID energy [eV]**	**Structure**	**Coverage**	**Number of *m/z* values assigned [%]**
933.3	100	Hex3HexNAc2	63.68	37.50
1095.4	100	Hex4HexNAc2	26.53	22.89
1419.4	120	Hex6HexNAc2	53.94	42.47
1581.5	150	Hex7HexNAc2	18.48	26.27
1743.5	150	Hex8HexNAc2	38.57	39.77
2028.7	200	Hex6HexNAc5	48.10	34.43
2341.8	200	Hex6HexNAc5NeuAc1	13.60	24.49
2393.8	200	Hex7HexNAc6	34.26	26.83

The individual fragment annotations (Figures SM1–SM8) clearly confirm the composition of the found N-glycans, but especially the identity of the high-mannoses since they exhibited the very characteristic signals belonging to their respective mannose groups.

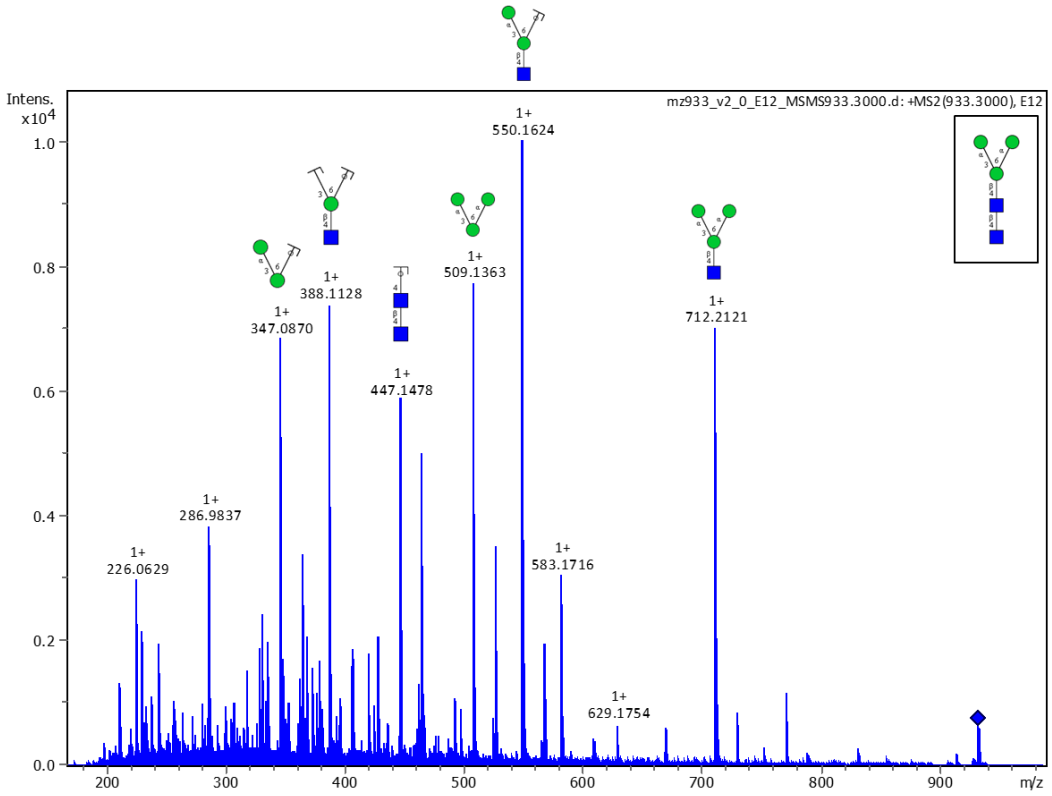

Figure SM1: MS/MS of m/z 933.3 -> high-mannose Man3. Note the characteristic signal at 509.1.

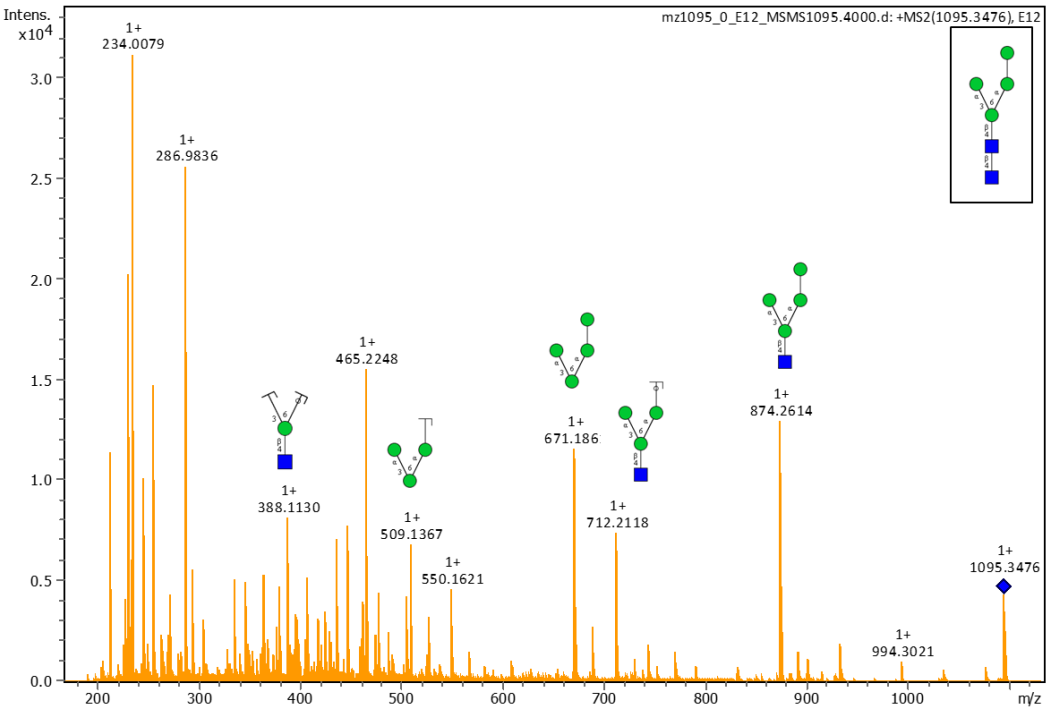

Figure SM2: MS/MS of m/z 1095.4 -> high-mannose Man4. Note the characteristic signal at 671.1.

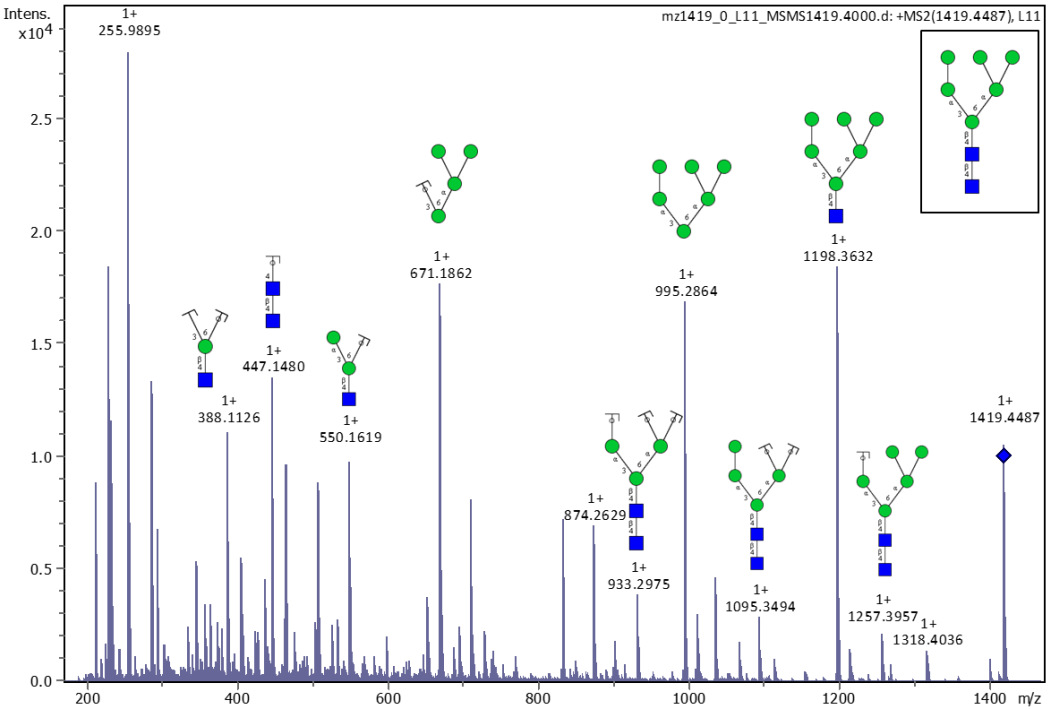

Figure SM3: MS/MS of m/z 1419.4 -> high-mannose Man6. Note the characteristic signal at 995.2.

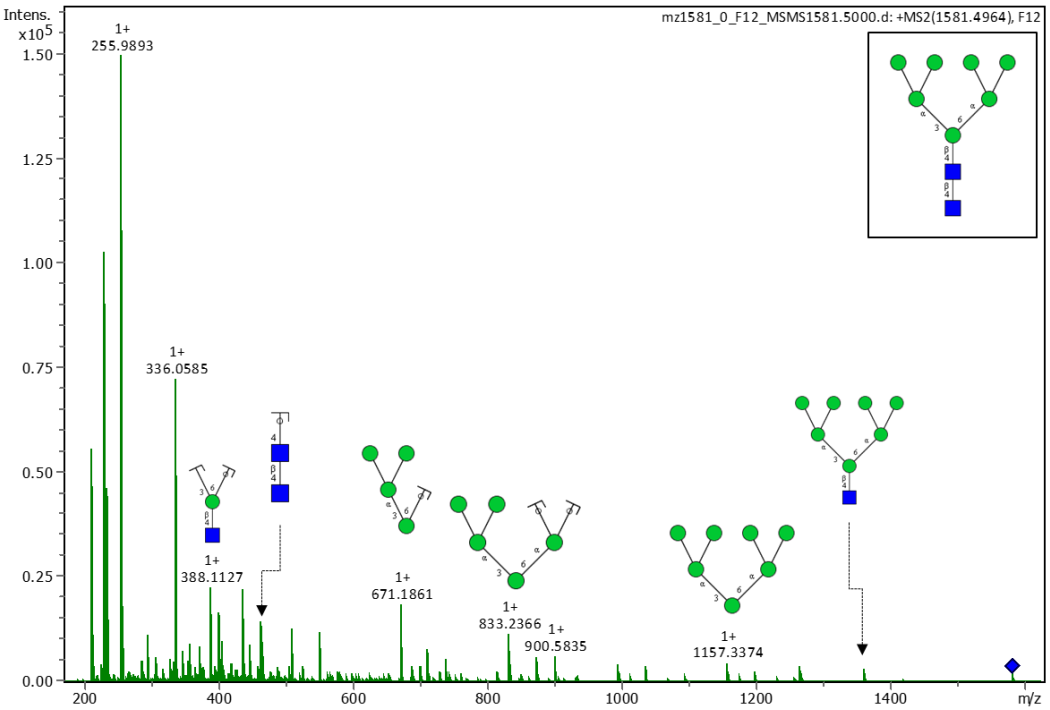

Figure SM4: MS/MS of m/z 1581.5 -> high-mannose Man7. Note the characteristic signal at 1157.3.

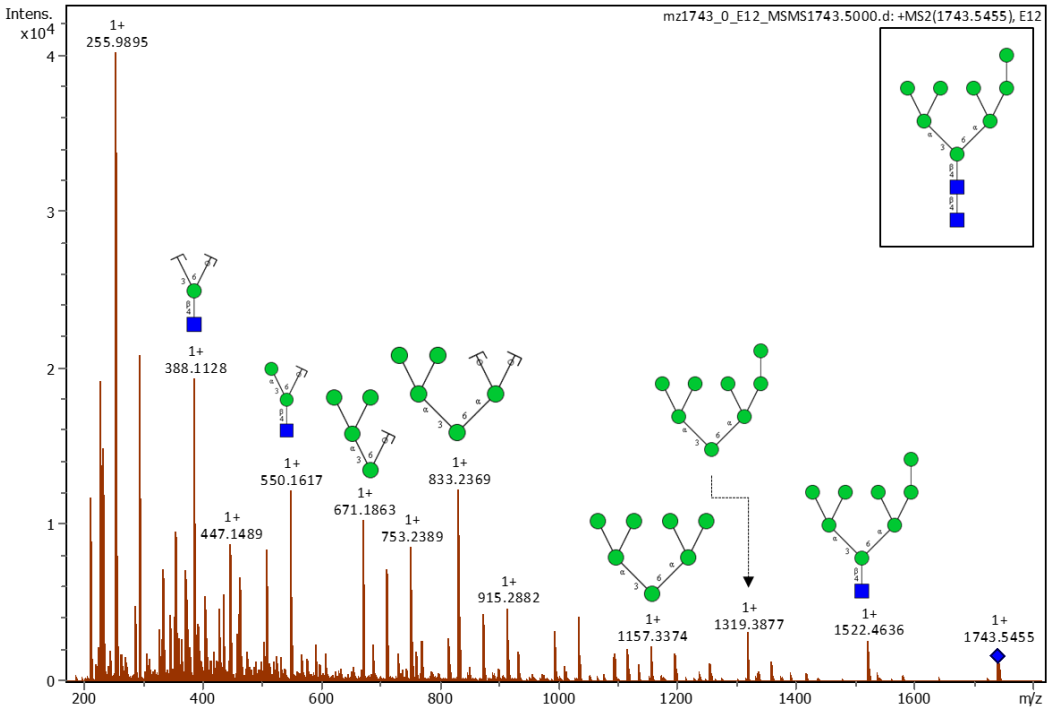

Figure SM5: MS/MS of m/z 1743.5 -> high-mannose Man8. Note the characteristic signal at 1319.3.

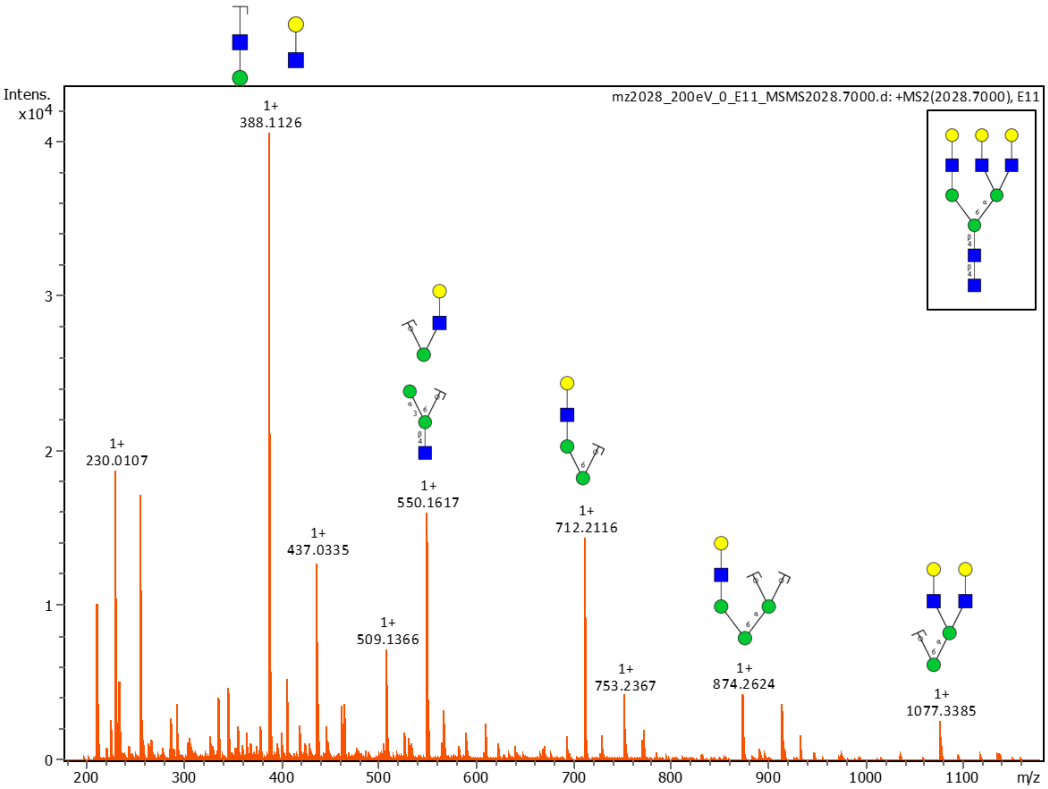

Figure SM6: MS/MS of m/z 2028.7 -> non-fucosylated tri-antennary complex.

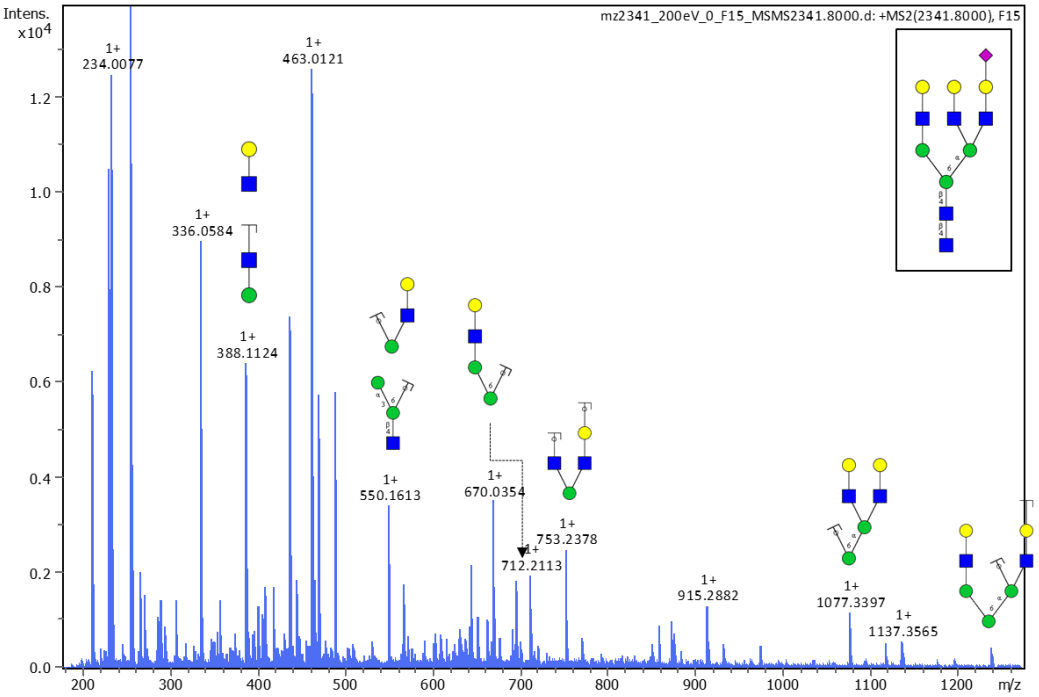

Figure SM7: MS/MS of m/z 2341.8 -> non-fucosylated tri-antennary complex with a single sialic acid. *Note that sialic residues are unstable and are therefore easily lost during or after ionization in a mass spectrometer.*

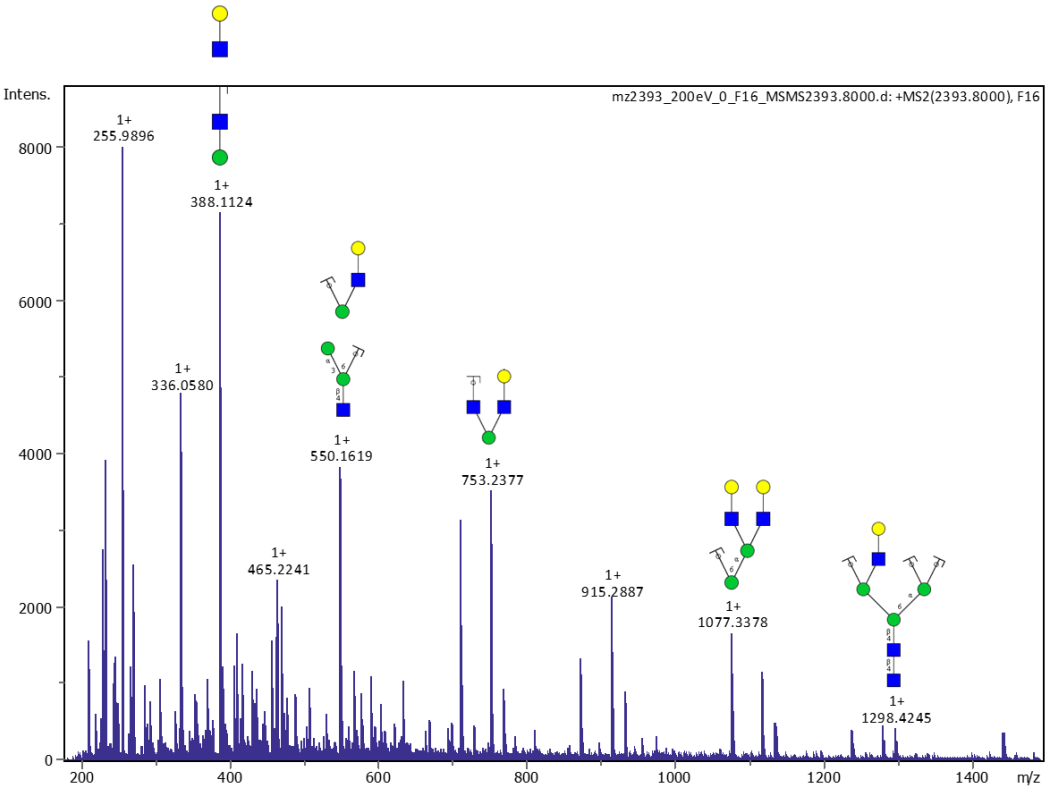

Figure SM8: MS/MS of m/z 2393.8 -> non-fucosylated tetra-antennary complex.

Even though the MS/MS experiments confirmed the major compositions of the glycans, they did not clarify their exact higher-level structure. We therefore prefer to not report or depict glycan structures in the main manuscript (see Table 1).

2. Glycan alterations in non-transformed and non-dysplastic tissue

It is known that cancer cells interact with their microenvironment, hence also with the surrounding non-transformed tissue. We have further investigated this idea by annotating all cases and sections for areas of already transformed but non-dysplastic epithelium (NDBE) and even completely untransformed squamous epithelium. 10 patients contained NDBE areas and 13 patients areas of squamous epithelium. Due to these small sample sizes we merged the categories “dysplasia” with “intra-mucosal neoplasia” and “esophageal adenocarcinoma” (EAC) with “metastatic EAC” to obtain three groups instead of five.

Using this division and the same statistical approach as described in the main analysis of the manuscript (repeated measurements ANOVA, corrected p-value threshold of 0.1), no differences in glycan intensities between the mentioned categories could be observed for untransformed squamous epithelium. However, when looking at NDBE areas, seven glycan signals demonstrated –similar to the findings reported in the transformed tissue– a continuous increase from NDBE to EAC (Figure SM9, Table SM3):

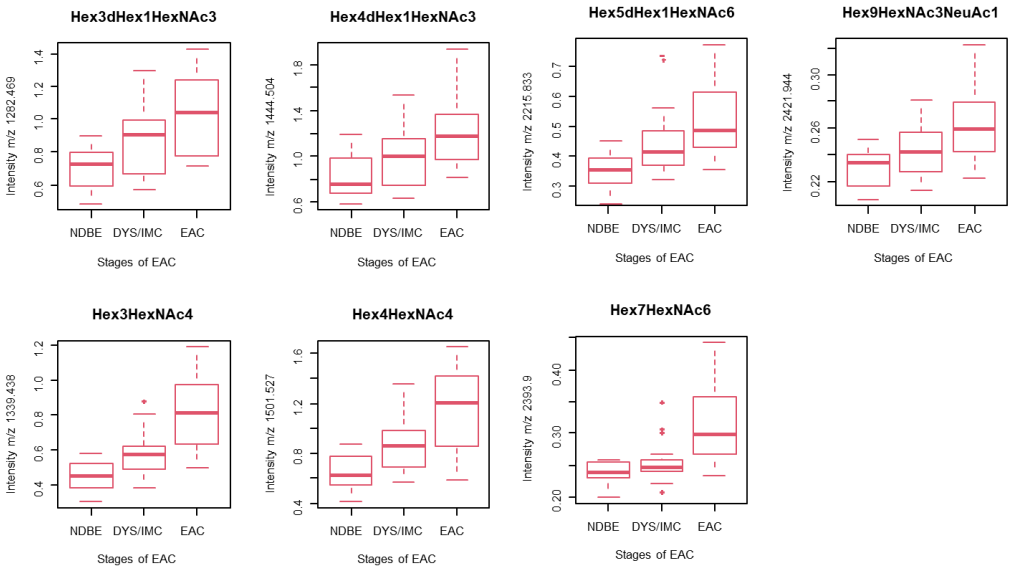

Figure SM9: Boxplots of seven N-glycans significantly altered in tissue areas of non-dysplastic Barrett's esophagus.

However there are some substantial differences in the type of glycans as compared to the analysis focusing on the transformed precursor/cancerous areas: there are no high-mannoses, but three fucosylated N-glycans and three hybrid N-glcyans amongst the seven altered signals (Table 1). The only overlap with the results of the manuscript is the non-fucosylated tetra-antennary complex (*m/z* 2393.90).

Table SM3: Significantly altered N-glycans in tissue areas of non-dysplastic Barrett's esophagus

Detected *m/z*	**Corrected ANOVA p-value**	**Glycan composition**	**Glycan type**
1282.47	0.061	Hex3dHex1HexNAc3	fucosylated hybrid
1339.44	0.061	Hex3HexNAc4	non-fucosylated bi-antennary complex
1444.50	0.019	Hex4dHex1HexNAc3	fucosylated hybrid
1501.53	0.061	Hex4HexNAc4	non-fucosylated bi-antennary complex
2215.83	0.075	Hex5dHex1HexNAc6	fucosylated tetra-antennary complex
2393.90	0.095	Hex7HexNAc6	non-fucosylated tetra-antennary complex
2421.94	0.061	Hex9HexNAc3NeuAc1	non-fucosylated hybrid with a single sialic acid

3. Power analyses

Power analyses can aid in finding out how many samples would actually be necessary to draw statistically more valid conclusion on the overall population of patients suffering from esophageal adenocarcinoma or precursor lesions thereof.

In order to do so we used the popular tool G*Power (v.3.1.9.7, available at: https://www.psychologie.hhu.de/arbeitsgruppen/allgemeine-psychologie-und-arbeitspsychologie/gpower) since it offers to perform power analysis for ANOVA with repeated measurements; as required in this case. The minimum power was set to 0.8, the number of groups

to 5, the number of measurements per sample to 4, and the average correlation between repeated measurements within a patient was determined to be 0.9828. The effect size had to be estimated for every mass channel separately (for practical reasons, we skipped every second channel) by calculating the mean intensity and standard deviation per group after log-transformation (Table SM4).

*Table SM4: Effect sizes as calculated by G*Power for every second mass channel*

Feature number	Group mean intensities	Mean of within-group standard deviations	G*Power effect size	G*Power sample size at alpha 0.1	G*Power sample size at alpha 0.05
933.33	0.1538	0.2895	0.9360	20	20
1095.37	-0.5824	0.2419	0.9470	20	20
1257.40	1.5001	0.4710	0.6022	35	40
1298.45	-0.4666	0.2974	0.4366	55	70
1419.44	1.2853	0.3551	0.6705	30	35
1460.48	-0.4892	0.3013	0.2296	190	230
1501.53	-0.4595	0.3403	0.4244	60	75
1581.52	0.5486	0.3733	0.7150	25	30
1622.52	-0.4234	0.3090	0.3270	95	120
1663.56	0.5519	0.4721	0.2922	120	145
1704.61	-0.5392	0.4174	0.6609	30	35
1793.64	-0.7466	0.2740	0.5206	40	50
1825.60	-0.8309	0.2932	0.4685	50	60
1866.64	-0.8562	0.3317	0.9482	20	20
1905.65	0.7204	0.3740	0.5778	35	45
1976.67	-0.1195	0.4905	0.2989	115	140
2012.70	0.4489	0.4836	0.2852	125	150
2053.74	-1.2672	0.2213	0.6446	30	35
2158.81	-0.4446	0.3985	0.3805	75	90
2199.80	-1.1760	0.2801	0.7055	25	30
2231.81	-1.3850	0.2756	1.1311	15	15
2304.87	-0.3768	0.4985	0.3830	70	90
2325.80	-0.9933	0.3190	0.2221	200	245
2361.89	-1.1189	0.3112	0.7175	25	30
2393.90	-1.4364	0.1439	0.9952	15	20
2435.88	-0.9850	0.2977	0.8153	20	25
2487.89	-1.0914	0.2180	0.5099	45	55
2523.98	-1.2250	0.3262	0.4522	55	65
2581.00	-1.5773	0.2867	0.5634	35	45
2686.07	-1.5835	0.1947	0.2706	135	170
2759.12	-1.5445	0.1382	0.5819	35	40
2853.12	-1.5713	0.1224	0.4483	55	65

Sample size calculations were performed for alpha=0.1 and 0.05. For alpha=0.1, this resulted in a minimum of 37.5 total samples (median over all channels; min=15; max=200). For alpha=0.05, 22.1% more samples were required on average (see Figure SM10-A): median=47.5, min=15, max=245.

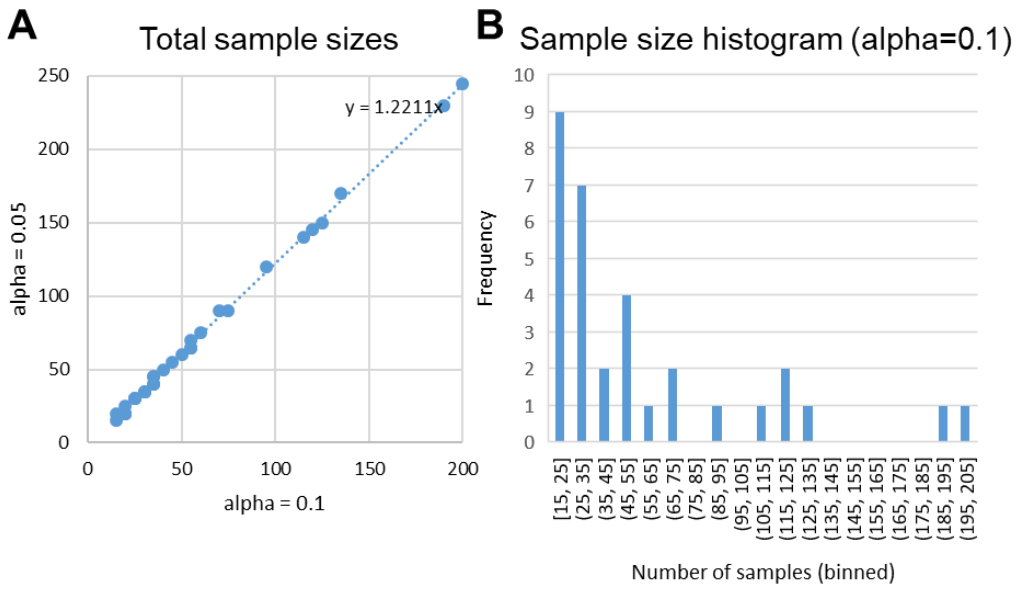

*Figure SM10: Total sample sizes necessary to obtain a statistical power of 0.8 according to G*Power calculations. A: Every data point in the graph corresponds to a mass channel. B: Histogram of sample size numbers for alpha=0.1.*

While these numbers are clearly beyond the total sample size used in this study, there is considerable variation in the number of necessary samples between the different mass channels. For instance, nine mass channels require less than 25 samples while six require more than 100 samples (Figure SM10-B). This is due to the relation between the actual biological effect (=intensity difference per group) and the masking of this difference by biological or technical variation. It is logical that this can vary for every glycan.

What has not been considered in these calculations is the *a posteriori* effect of the multiple-testing correction, which also leads to an additional increase of the number of samples. Some simulations using the strict and straight-forward-to-calculate Bonferroni correction, indicate that the numbers would have to even double (with a maximum alpha = 0.1/64 mass channels = 0.0016). However, in the current study we used the less-strict and more popular Benjamini-Hochberg procedure, which is computationally less predictable. Hence, we speculate that one would need 150% of the recommended samples by G*Power.

In conclusion, if one would want to make sure that this holds for 80% of the mass channels, in total 137 samples (~27 samples per group, or seven times more than in our study) would need to be involved in a study where the statistical reliability would be at the core.